

NUMERICAL SIMULATION OF RESIDUAL STRESS IN PIPING COMPONENTS AT FRAMATOME-ANP

Philippe Gilles

FRAMATOME-ANP, Tour AREVA

92084 Paris la Défense, France

Phone: 33 1 4796 1677,

Fax: 33 1 4796 2934

E-mail: philippe.gilles@framatome-anp.com

Christian Franco

FRAMATOME-ANP, Tour AREVA

92084 Paris la Défense, France

Marie-France Cipièrè

FRAMATOME-ANP, Tour AREVA

Pascal Ould

FRAMATOME-ANP, Tour AREVA

ABSTRACT

Numerous manufacturing processes induce residual stresses and distortions in piping components and associated welds: quenching of cast pipings, machining and welding. In Pressurized Water Reactors, most of the components have a large thickness for sustaining pressure and distortions are a minor source of concern. This is not the case for residual stresses which may have a strong influence on several type of damage such as fatigue, corrosion, brittle fracture. In low toughness components, residual stress fields may contribute to ductile tearing initiation. These potential damages are mitigated after welding by stress relief heat treatment, which is applied in a systematic manner to ferritic components of the primary system in nuclear reactors. This treatment is not applied on austenitic piping for which the heat treatment temperature is limited due to the risk of sensitization and residual stresses are difficult to eliminate completely.

Since on site measurements are costly and difficult to perform, numerical simulation appears to be an attractive tool for estimating residual stress distributions. Framatome-ANP is working on modelling manufacturing processes with that purpose in mind. This paper presents three kinds of applications illustrating efforts on welding, quenching and machining simulation. First a comparison is shown between computations and measurements of residual stress induced by welding of a dissimilar weld metal junction. Then numerical simulations of quenching of a cast stainless steel nozzle are presented. Finally quenching followed by machining and grinding of this cast component are considered in a full simulation of the manufacturing process. Computed distortions and residual stresses are compared with experimental measurements at different stages of the manufacturing process.

Keywords: Numerical Welding Simulation, Numerical Machining Simulation, Finite Element Computations, Elastic-Visco-Plastic Behavior, Residual Stress.

1. INTRODUCTION

Residual stresses present in Pressurized Water Reactors do not constitute a major problem at the design stage. They do, however, strongly impact some types of damage – specifically fatigue crack and corrosion crack initiation and growth (Fricke *et al.*, 1998, Gilles, 2002). However stress relief heat treatment is not applied on stainless steel pipes and the 600°C post weld heat treatment of bi-metallic welds is not completely efficient. Furthermore, through-thickness measurement of residual stress is not feasible on-site. Numerical simulation of the welding process is, in most of the cases, the only way to obtain residual stress fields and therefore improve the accuracy of defect assessments.

Most of the manufacturing processes, like quenching, welding, machining as well as welding repairs do generate residual stresses. These stresses may play different roles on damage depending whether they are local or global. All thermal process such as welding or quenching, produce residual stress fields throughout the component thickness and may play an important role in fatigue propagation and brittle fracture. Conversely, machining and grinding induce high residual stress gradients close to the surface and have a dominant influence on stress corrosion or fatigue crack initiation. It is therefore important to know the origin of residual stress fields and the most reliable way to reproduce numerically these fields consist in simulating the whole manufacturing process. This is the orientation of FRAMATOME-ANP R&D efforts, which begin to bring some success in industrial applications described below.

2. NUMERICAL SIMULATION OF WELDING

Framatome-ANP has been working on numerical simulation of welding since more than 25 years (Gilles, 2004). The worldwide known SYSWELD® code is born in Framatome-ANP, but the largest part of Framatome-ANP experience in this field relies in the numerous studies performed by German and French teams on industrial components. We present in this paragraph a large part of FRAMATOME-ANP efforts devoted to welding simulation of a dissimilar weld metal junction.

2.1. The Dissimilar Weld Junction problem

In most of nuclear reactors, heavy section components made in low alloy steel are connected with stainless steel piping systems. The junctions are performed between ferritic nozzle ends and austenitic stainless steel piping, following a special manufacturing procedure to ensure a good resistance of the joint. Two types of joining procedures may be used: the old practice consists in buttering the ferritic end with layers of austenitic stainless steel and then joining the pipe sections with an austenitic stainless steel filler metal is used. Now a TIG (Tungsten Inert Gas) narrow gap welding with a nickel base alloy as filler metal joining directly the ferritic nozzle to an austenitic stainless steel safe end is preferred. Post weld heat treatment (PWHT) is applied to reduce residual stresses in the heat affected zone (HAZ), but whatever the process is, the difference in thermal expansion coefficients induces residual stresses during the cooling stage. Furthermore, differences in tensile properties may cause strain concentration at the weld to ferritic steel interface which enhances the risk of crack initiation and extension.

Dissimilar Metal Weld junctions (DMW) have been a subject of concern in few plants when corrosion cracks have been discovered in stainless steel DMWs (Cattant, 1994) and nickel base alloy ones (VC Summer, Ringhals). In a more general way, the integrity of aged DMWs constitutes an important safety issue (EUR20281, 2001).

Two EC projects BIMET (Chas, 2001) and ADIMEW (Faigy 2001 & 2004) have been conducted on DMW ductile fracture behavior. Namely, the ADIMEW (*Assessment of aged piping DIssimilar MEtal Weld integrity*) project aimed to quantify the accuracy of structural integrity procedures used in the European nuclear industry to ensure the safety of defect-containing dissimilar metal weld junctions in aged PWR Class 1 piping. A 16 inch diameter DMW weld junction containing a large machined crack has been tested successfully under bending at 300 °C to determine the actual behavior of cracks close to the interface. Test results and fracture analyses of ductile tearing behavior have been presented at the PVP 2004 conference (Martin, Wintle, Gilles, 2004).

Dissimilar Metal Weld junctions exhibit very strong residual stress fields in as-welded condition, but also after Post Weld Heat Treatment (PWHT). The knowledge of residual stress fields is of importance in integrity analyses especially in aged junctions. As a side project, detailed measurements of the residual stress fields in the components were performed on BIMET and ADIMEW pipe junctions. The next paragraph present numerical computations of the residual stress fields computations conducted by FRAMATOME-ANP on the ADIMEW mock-up.

2.2. Numerical simulation of the welding of a large diameter DMW

In the ADIMEW programme, two 16" Dissimilar Metal Weld mock-ups were manufactured by FRAMATOME-ANP. After machining and PWHT the external diameter of these mock-ups became 453 mm and their thickness 51mm. One was cut-up to measure welding residual stresses and to provide small-scale specimens for measurement of tensile and fracture toughness properties of the constituent parent steels, weld metals and associated heat affected zones. The second mock-up was used for the actual pipe test (Martin, 2004). The 2 Dissimilar Metal Weld mock-ups were manufactured in 5 steps (partly shown in Fig. 1b):

- 4 layer buttering (309 & 308L) and machining

- Vee groove 308L welding
- Stress relief
- Outside & inside machining

Complementary measurement techniques were applied to determine as accurately as possible the residual stress fields in the weld and the Heat Affected Zone (HAZ). Particular emphasis was on the through wall residual stress distribution in the area of the ferritic steel – austenitic stainless steel weld interface. The Neutron Diffraction (ND) technique has been applied by the Institute of Energy (IE-JRC) to determine the residual stress fields non-destructively and through thickness. Measurements were performed at various locations within the weld, the buttering layer and base materials in three orthogonal directions, i.e., the component hoop, axial and radial directions. Details may be found in (Ohms, 2004). TWI performed Hole Drilling measurement (HD) at ten locations on the outer wall, and at four locations on the inner wall.

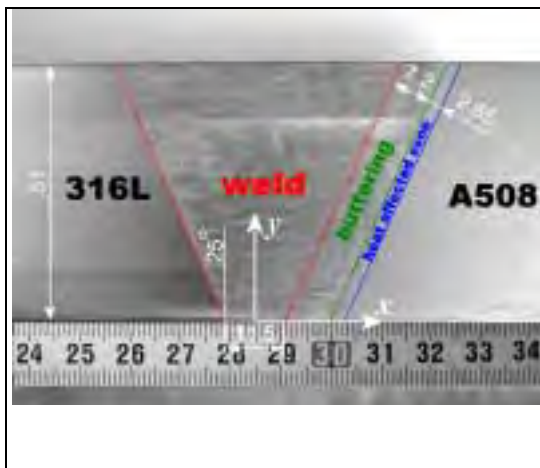


Fig. 1a Trough thickness macrograph

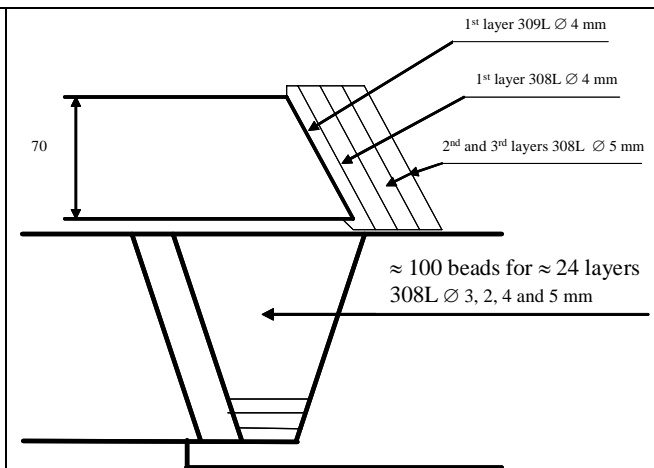


Fig. 1b: 2 main steps : buttering and filling

Since a large difference has been observed between these two measurements (Fig. 2a), MatTec Laboratory proposed using the cut compliance technique (Schindler, 2003). These measurements (Fig. 2b) show that the compressive stress on the surfaces is a purely local effect. Beneath the surfaces the stresses revert to those consistent with measurements made by JRC and calculated by Framatome-ANP. The volumetric sensitivity of neutron radiography measurements and finite element calculations would not have been capable of identifying a local stress within a few millimeters of the surface.

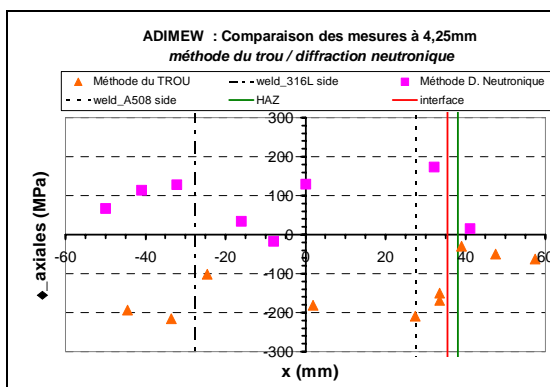


Fig. 2a Hole drilling axial residual stress measurements (triangles) at the outer surface and neutron diffraction measurements at 4.25 mm in depth (squares)

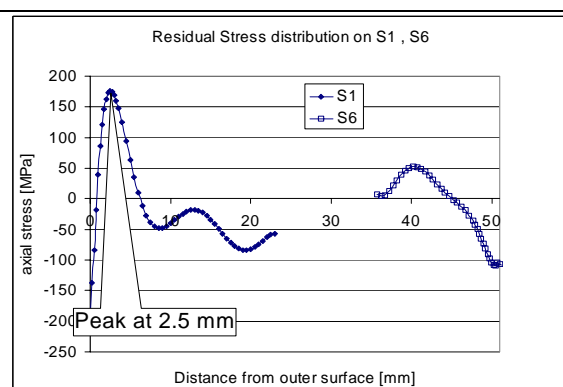


Fig. 2b Cut Compliance axial residual stress measurements in the middle of the weld

The differences between HD measurements and extrapolation of ND measurements on the walls are attributed to machining. The heating due to machining may induce considerable compressive stress on a thin layer under the surface. This effect has not been modelled in the ADIMEW residual stress simulations.

Framatome-ANP has performed the three following calculations:

- A simplified analysis, which consists of a cooling calculation from an assumed stress-free state after the stress-relief heat treatment.
- A detailed macrobead analysis. Each elementary step of the mock-up manufacturing procedure is simulated, but the welding is modelled by deposition of layers grouping all the beads lying in a same plane. This macrobead technique has been validated on detailed welding simulations of a thirteen pass welding of two austenitic stainless steel pipes.
- A detailed pass by pass analysis in which all the steps of the procedure and the deposit of all the beads are simulated. The thermal field is obtained by 3D computation on a plate with a source calibrated for each welding step.

These computations are 2D axisymmetric and the self restraint is accounted for by fixing appropriate boundary conditions. Three materials have been characterized: A508 for ferritic base metal, 316L for austenitic base metal, and 308L for weld metal. The buttering was considered as identical to the filler weld material. For the weld metal, physical characteristics and stress-strain curves have been obtained from measurements at 20°C and 300°C, RCC-M (2000) material data base for current temperatures and extrapolations using a private data base. We may conclude from comparisons (some of these being presented in Figs. 3 and 4) between computed and measured residual stress that:

- The simplified analysis (Fig 3a) gives much lower hoop stresses than measured and computed results, showing that PWHT cannot relief the hoop stresses. The relief is more efficient on axial stresses.
- The macrobead simulation gives similar results than the pass by pass computation in the upper part of the weld, but underestimates the stresses at the root pass. These differences are probably due to a weakness of the macrobead technique when applied to the buttering.
- The pass by pass analysis is in excellent agreement with the measurements. According to IE-JRC, hoop stress measurements are more reliable and some measurements in the middle of the weld are not accurate due to the high texturing of the weld.

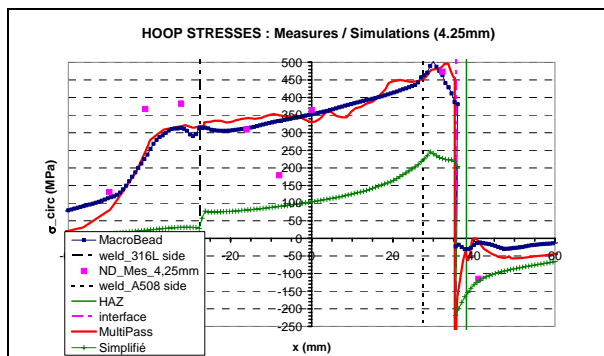


Fig. 3a Computed and measured hoop stresses at 4,25 mm from the outer wall

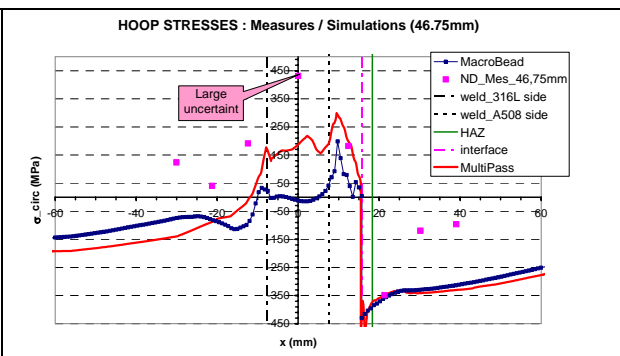


Fig. 3b Computed and measured hoop stresses at 4,25 mm from the inner wall

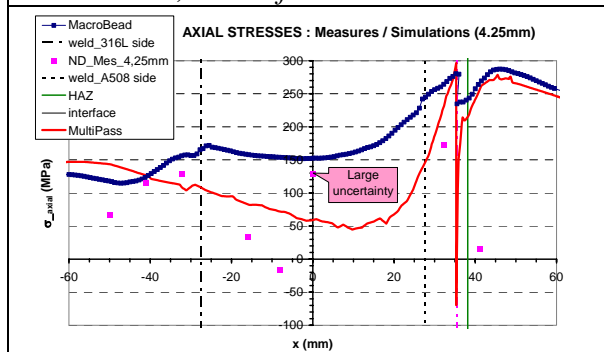


Fig. 4a Computed and measured axial stresses at 4,25 mm from the outer wall

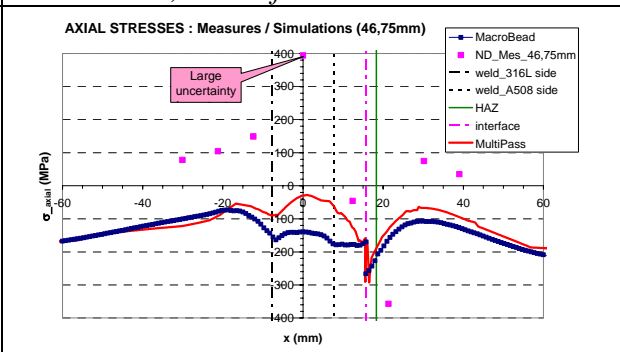


Fig. 4b Computed and measured axial stresses at 4,25 mm from the inner wall

3. NUMERICAL SIMULATION OF QUENCHING

Cast components made of duplex stainless steel are used in the primary system of Pressurized Water Reactors. These austeno-ferritic stainless steel components are susceptible to thermal aging embrittlement and they contain small shrinkage cavities due to the manufacturing process. Even if the behavior of aged austeno-ferritic stainless steel components remains ductile, their toughness decreases and residual stresses are likely to contribute to tearing initiation. The cast stainless steel components are delivered in the as quenched condition. This annealing heat treatment induces high level of residual stresses. Some cast stainless steel are submitted to a stabilizing heat treatment at 400°C (e.g. pump casing) which removes peak stresses but the complete removal of the residual stress on this cast austenitic stainless steel can only be obtained by treatments at higher temperatures which are not recommended due to the risk of sensitization. Therefore residual stress fields have been taken into account in integrity analysis, the problem being how to account for residual stress fields in numerical analyses. Two types of residual stress computations were conducted by FRAMATOME-ANP: an empirical approach in which measured residual stress fields were reproduced through a thermoelastic computation and a direct simulation of the quenching process.

3.1 Empirical residual stress simulation

To simulate the presence of these residual stresses, a radial distribution of temperature which generates thermal stresses close to the measured residual stress (or theoretical as in Fig. 5) profile. This type of fit is much better than a simple polynomial fit for two reasons: the thermal stress functions are more suited than a polynomial fit to represent residual stress distributions and only one type of stress distribution is needed (axial or circumferential). This approach was developed by Framatome-ANP within the framework of the analysis of a burst test of a tin in the presence of residual stresses. This method gives satisfactory results for a field of stresses generated by the water quenching, as it is shown in Fig. 5 for a ring. The following residual stress profile is obtained:

- Finite Element longitudinal and circumferential stresses identical,
- tensile stress at mid-thickness,
- compressive stresses at the outer and inner surfaces.

The same approach has been applied to 3D models of cracked elbows.

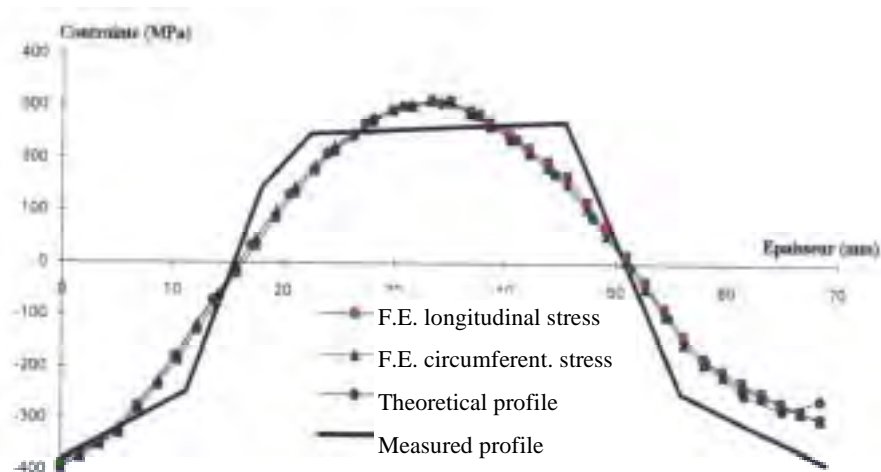


Fig. 5. Residual stress profiles through the thickness of a ring: measurement and axisymmetric computation fitted on a theoretical profile

This approach is limited to the geometries on which stress measurements have been performed. However experimental results have shown that residual stress profiles induced by quenching on elbows are close to those found on straight pipes. The measurements throughout the wall thickness used as reference were performed using the block removal and layering technique. In this technique blocks are first cut out of the component and the relaxation of the strain in the blocks are measured with strain gages stuck on the surface of the blocks. Then the distribution of stresses parallel to the surface is measured through the thickness with the layering method consisting in following on one side of the block the evolution of the strain when removing material from the

opposite face (Legatt, 1978). This approach has been used to check the effect of residual stress fields on the crack driving force J. The influence of residual stresses on the crack extension force J, becomes negligible when the cracked ligament has been yielded completely, that is when the applied load exceeds the limit load of the cracked cross section (Gilles, 2002).

3.2. Direct simulation of the residual stress fields induced by quenching

Numerical simulations of the quenching process have been conducted on cast stainless steel elbows and nozzles. The elbow computations have shown that residual stress profiles are quite similar in pipes and elbows of identical cross section (Dupas, 1986). In the case of a 12” inclined nozzle, the empirical approach was unthinkable; therefore a detailed simulation of the quenching process has been conducted.

These nozzles have been cast in one piece and then were submitted to an annealing heat treatment. This treatment consist of heating up to 1120°C, maintaining this temperature for 8 hours and then quenching by diving the part in water at room temperature. This heat treatment allows eliminating all the precipitates and phases formed during the slow cooling of the solidification process. Then the component is machined to its design dimensions. The inner and outer walls of the nozzle areas which have not been machined have been grinded by successive steps up to 5 or 10 mm.

Material characteristics were determined between 20°C and 1200°C from some data on austenitic-ferritic stainless steels available in the literature, and data on austenitic stainless steels issued from standards (RSEM, 1997) and in-house characterizations. For thermal expansion coefficient and density of the cast stainless steel, corrections have been on austenitic stainless steel values to take into account the ferrite content. An important work has been made for determining tensile stress-strain curves. The tensile stress-strain curves at 20°C and 350°C of the cast stainless steel issued from RSEM have been lined up with the values measured in the acceptance tests-(309 MPa at 20°C, 218 MPa at 340°C) and between these temperatures linear interpolation has been applied on stress/yield stress ratio values at given plastic stain value. For temperatures higher than 340°C, the yield stress variation with temperature has been derived from results on grade Z2.CND.17-12 nitrogen strengthened austenitic stainless steel. Between 350°C and 1000°C, the stress-strain curves are derived from the curve at 350°C, results of in-house characterisation and a scaling technique on stress/yield stress ratio values. Beyond 1000°C, a linear strain hardening has been considered.

The main problem encountered in the quenching simulation was the determination of the heat exchange coefficient. Natural convection has been considered from 20°C to 105 °C. At higher temperatures, the selected heat exchange coefficient values are those obtained in an experimental study of steel pipe quenching.

Temperatures (°C)	20	30	40	110	267	467	1120
Heat exchange coefficient (W/m ² .°C)	0	559	625	1600	6000	6000	1500

Table 1: Main variations of the thermal exchange coefficient

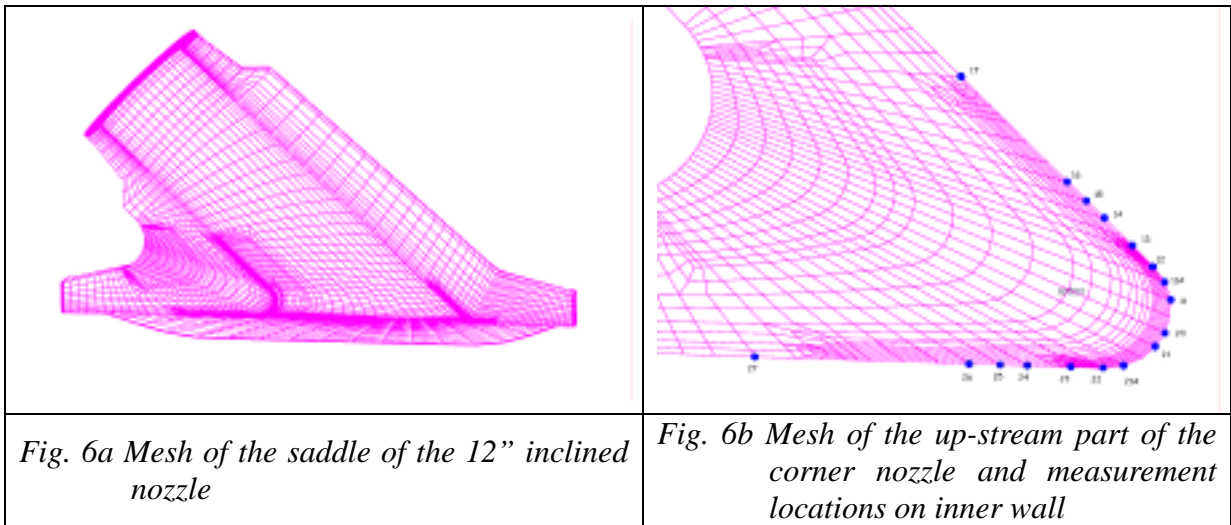


Fig. 6a Mesh of the saddle of the 12” inclined nozzle

Fig. 6b Mesh of the up-stream part of the corner nozzle and measurement locations on inner wall

For symmetry reasons, half a nozzle has been modelled. Temperatures have been computed on a linear mesh while thermomechanical computations were conducted on a quadratic mesh containing 4214 elements (Fig. 6a).

The quenching has been modelled as a one second thermal shock from 1120°C to 20°C applied on the whole nozzle followed by a hold-down at 20°C. Temperatures have been computed considering non linear temperature dependence of the material characteristics and very fine steps have been considered at the beginning of the shock. Very strong temperature gradients appear on few millimetres under the surfaces up to 500s. Then, the whole nozzle, except the very thick upstream corner area is cooled down. In that area, temperature profiles are non symmetrical in the thickness as in pipe sections.

The thermoplastic incremental computations were conducted using a von Mises isotropic yielding model and considering a small displacement hypothesis. The machining and grinding processes have been simulated by setting down the Young's modulus value to zero at the end of the thermoplastic computation. On the inner wall this procedure has been applied in three steps on the three layers of elements. The residual stress fields do correspond to the end of this final part of the simulation. Close to the wall and in the mid thickness zone, the material has been yielded. In all trough thickness sections, the stress distributions are typical of those found on structures under thermal shock: all shear stresses are zero (therefore axial and circumferential stresses are principal stresses). Radial stresses trough thickness are close to zero, except in zones where cross section shapes are changing fast as in the corner area.

Special attention has been paid to the residual stress profile in the corner nozzle, area of high stress concentration under in-service loadings. On a scale 1 mock-up residual stress measurements were performed by TWI using the surface Hole Drilling method, giving residual stresses at a depth of 0.5 mm below the surface. We will concentrate on results relative to the up-stream part of the nozzle corner. Figure 7 compares measured and computed stress profiles on the inner wall.

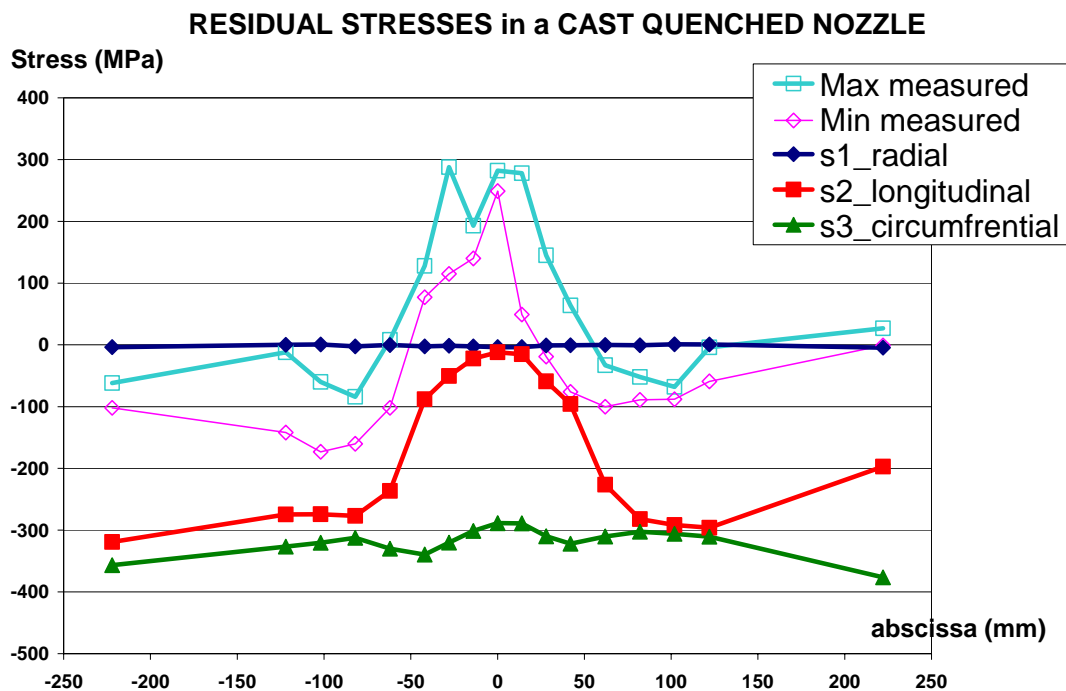


Fig. 7 Measured and computed principal stresses as a function of the curvilinear abscissa along the up-stream nozzle corner

The maximum measured values have to be compared to the computed longitudinal stresses, which presents the same profile, but with values lowered almost by 300 MPa! The minimum measured values corresponding to the circumferential direction have a bell-shaped profile like the measured longitudinal stresses but which differs totally from the flat profile of the computed circumferential stresses. The computed circumferential stress values are lying between -300 and -400 MPa, but the measured corresponding vales in the corner are highly tensile! On the downstream corner area, measured and computed stress profiles are similar, but a same difference of about

350 MPa is found. Some measurements have been made far from the corner area and their values were also about 300 MPa higher than the computed values in both directions.

A lot of care has been taken in determining material properties and in boundary conditions. However due to a lack of data, the strain hardening has been considered as isotropic (which may explain the high level of computed stress absolute values) and the heat exchange coefficient deduced from a pipe quenching test. Therefore, a detailed sensitivity analysis was conducted on the heat exchange coefficient variations during quenching and on the type of cyclic strain hardening (isotropic or kinematic). The value of the heat exchange coefficient h has a strong influence on the residual stress level (Fig. 8a), but out of the corner zone! In the current zone, a low h value which could be representative of a film boiling phenomenon reduces the difference between computed and measured stresses. However the computed circumferential stress profile remains flat and the values are even 50 MPa higher than that obtained with a high h value. The computational results obtained with a kinematic strain hardening hypothesis reduces the gap with the measured values (Fig. 8b), and this is also true in other zones. However, computed residual stresses at the inner surface are highly compressive and on the upstream corner, the computed circumferential stress profile does not match at all the measurements.

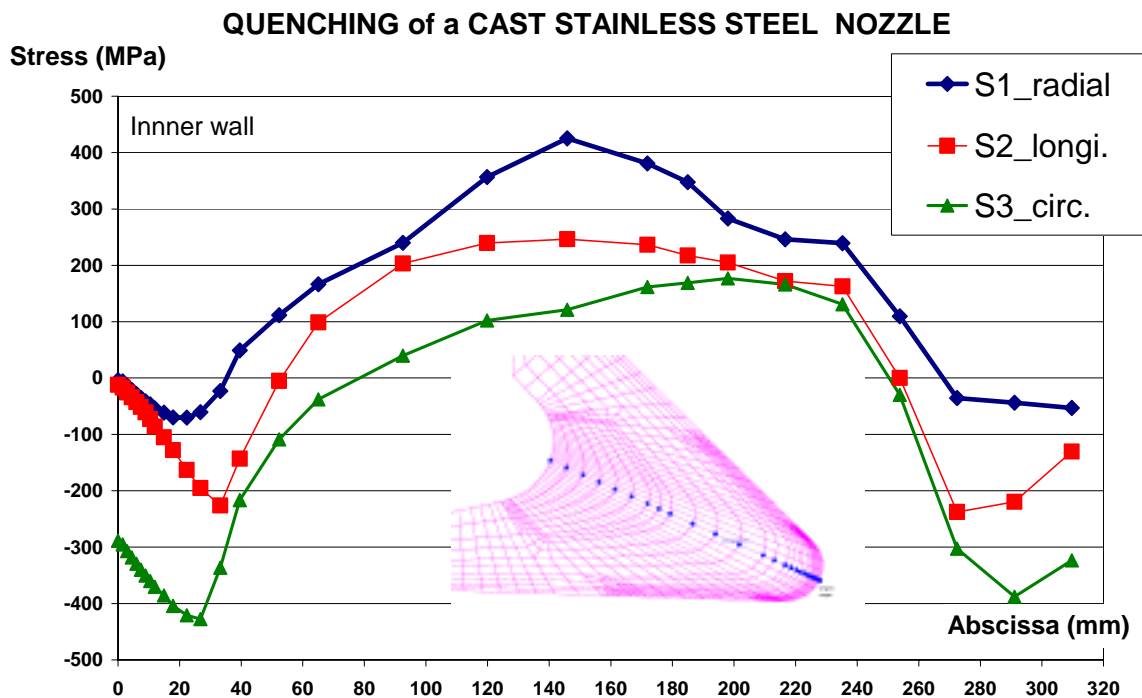
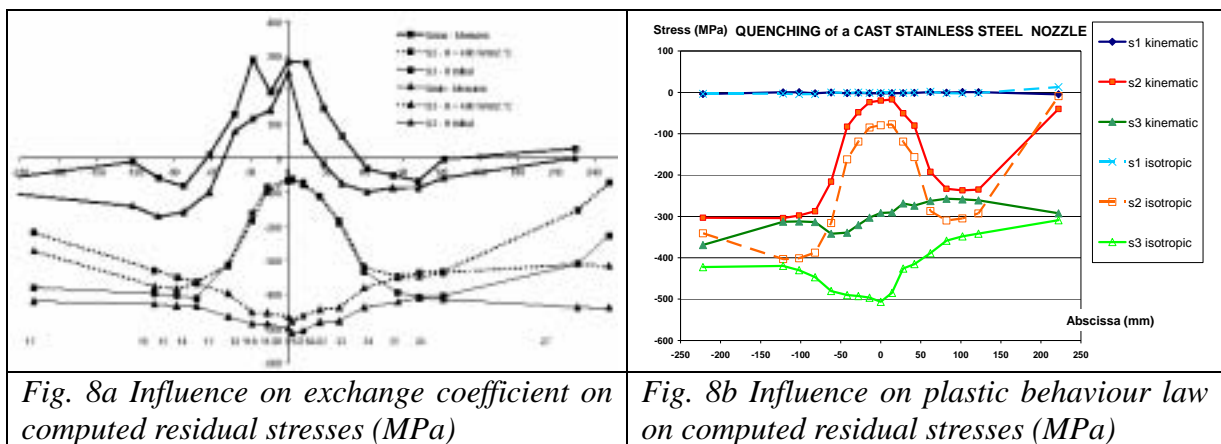


Fig. 9 Computed principal stresses distribution through the thickness in the up-stream nozzle corner cross section

Figure 9 shows that on the inner wall, computed residual circumferential and longitudinal stresses are compressive over about 60 mm, like observed on pipes and elbows.

In a previous study on residual stress induced by quenching in a duplex cast stainless steel pipe a reasonably good agreement had been obtained in the pipe thickness between measured and computed hoop stresses. The quenching parameters considered in the analysis were nearly the same than those of the cast nozzle and destructive measurements had provided the trough thickness stress profiles, which was in total disagreement with surface hole drilling residual stress measurements. Therefore finer removing of material for the stress profile measurements were decided (Faure, 1996) and their results evidenced the existence of a very steep stress gradient on 1 mm below the surface from 180 MPa to -165 MPa on the surface. The simulation of quenching and machining had been unable to deliver such a gradient, but the quenching simulation gave rather satisfying results. For the nozzle, trough wall measurements have not been made, therefore only a more representative computation of residual stress induced by machining could explain the observed discrepancies. This study is presented in the following paragraph.

4. NUMERICAL SIMULATION OF MACHINING AND GRINDING

Sensitivity analyses on quenching simulation could not explain the large discrepancy found on the nozzle corner inner surface between measured tensile residual stress distributions and computed compressive residual stress distributions. To resolve this problem is important for example to know what values have to be taken into account in fatigue analyses, and especially to validate the simulation of the manufacturing process.

4.1. Numerical simulation of heat input due to machining

Observations made on the influence of surface treatment on residual stress fields have shown that grinding such as applied to the nozzle corner, induces tensile residual stress in the thickness up to a 5 mm depth. This grinding is characterized by a significant heating up. This heat input is ignored in simulating machining by a simple material removal. The new simulation of the nozzle manufacturing; contains three phases:

- Simulation of the quenching by a steep cooling shock as detailed in the previous paragraph, but using a kinematik strain hardening model.
- Simulation of the heating up induced by the machining process by applying a hot thermal shock.
- Simulation of the material removal by decreasing to zero the Young's modulus value.

The temperature gradient and the thermal shock location have been fitted to reproduce the surface stresses measured on the nozzle corner. For the machining out of the nozzle corner area a 2 seconds temperature increase from 20°C to 75°C followed by a 2 second cooling down to 20°C have been applied on the whole inner surface of the nozzle. The heating up due to grinding in the nozzle area is modelled by a 2 second heating from 20°C to 175°C followed by a 2 second cooling down at 20°C in a 69 mm large band as shown on Figure 10.

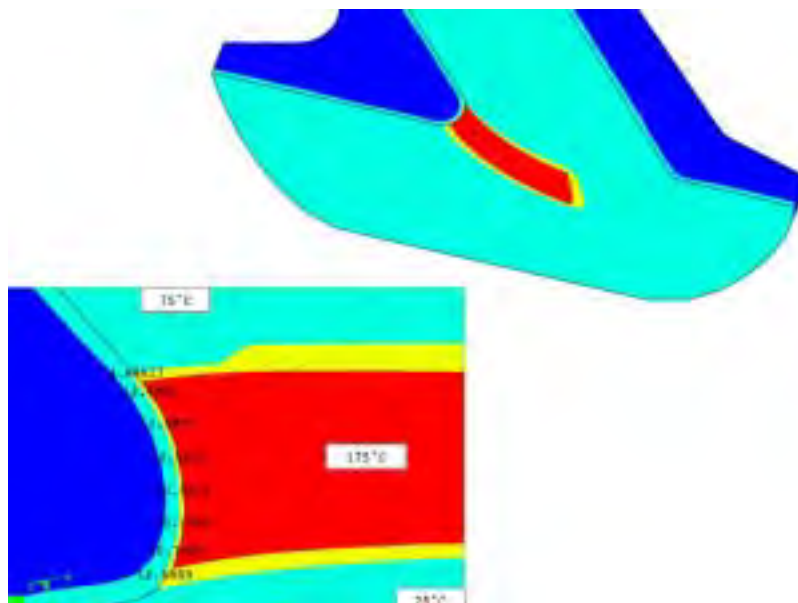


Fig. 10 Location of the temperature gradients used in the grinding simulation

The changes on the residual stress fields induced by the heating-up on the surface of the up-stream corner are illustrated on Figure 11. The stress level is increased by 200 to 300 MPa in the corner area. The increase is higher in this area where the applied temperature gradient is higher, which do correspond to the difference in grinding process in that area. The good correlation with the stress measurements observed in Figure 13 shows that the fitted values of the thermal gradients and of the zones of application are appropriate. The results obtained on the down stream of the nozzle are not presented here, since no correction accounting for the heating-up as been applied to this zone. In this area, stress relief occurs, but the agreement with measured stresses is poor even if the discrepancies are much lower than without applying any heating-up on the surfaces.

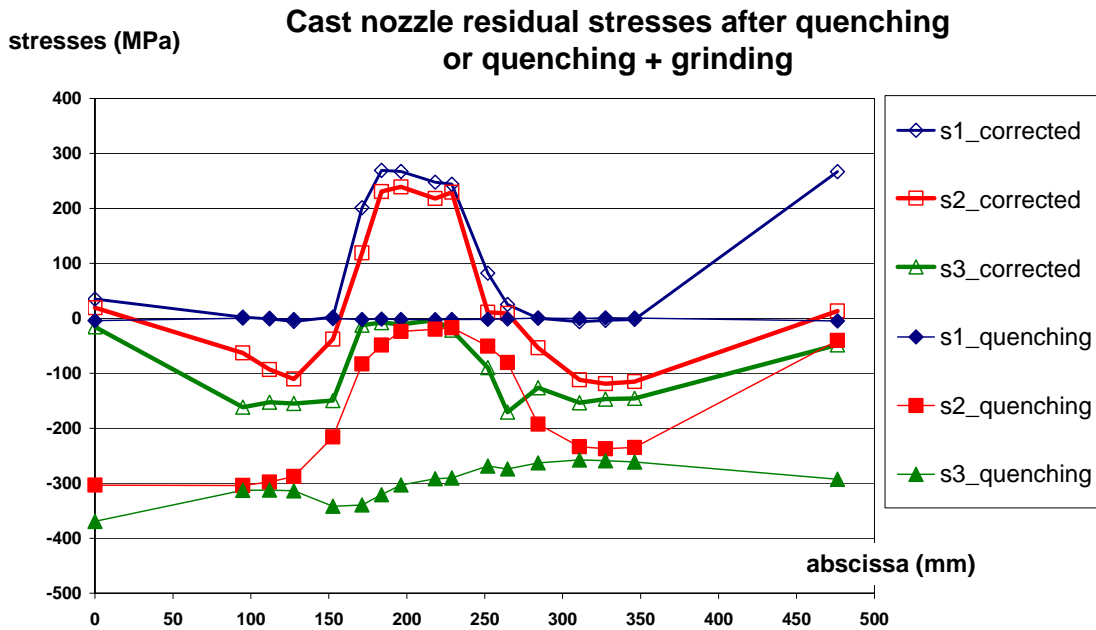


Fig. 11 Influence of the heating-up induce by grinding on residual stresses in the inner wall of the up-stream part of the nozzle

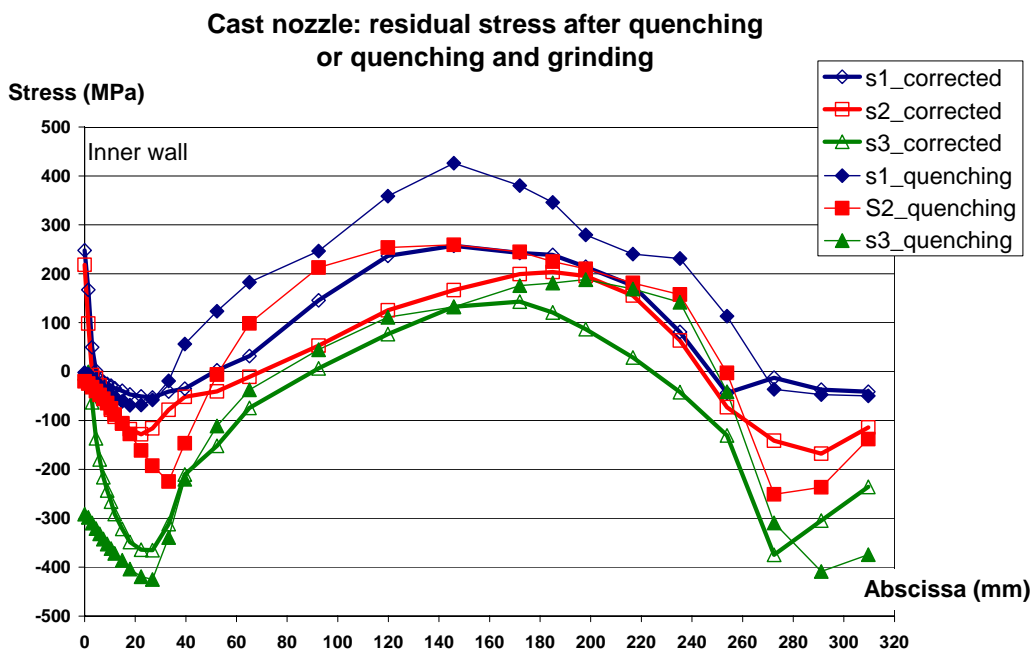
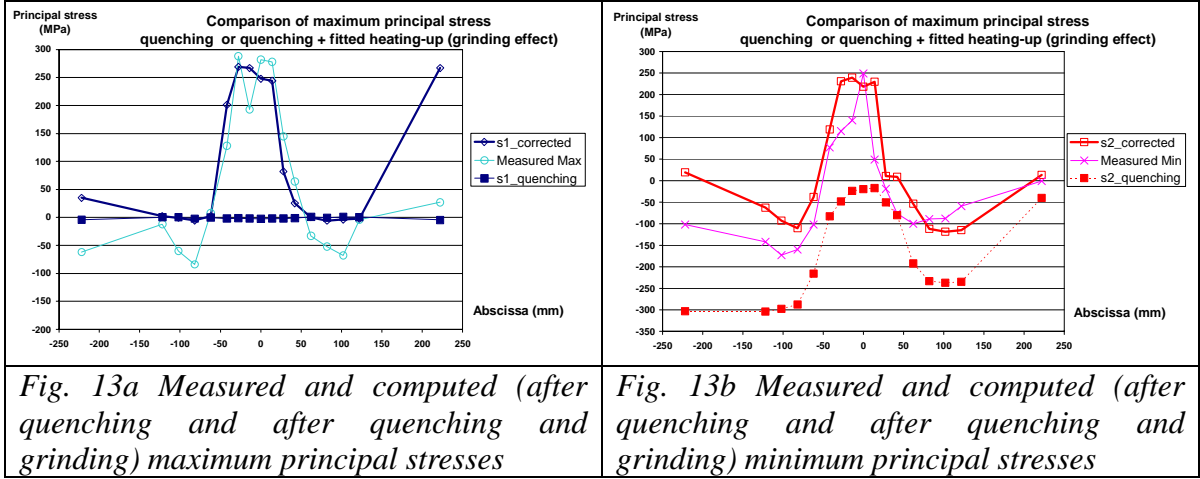


Fig. 12 Influence of the heating-up induce by grinding on residual stresses distributions through the thickness in the up-stream nozzle cross section

The applied hot thermal shocks give tensile residual stress fields in the thickness on the 5 first mm below the surface in the up-stream nozzle cross section (Fig. 12) as observed in grinding experiments. It may be seen on this figure, that the heating-up at the surface reduces the tensile stresses. However, the stress profile remains of the same type. This reduction of the residual stress level corresponds to a stress relaxation. This relaxation reduces also the distortions of the nozzle.



These figures show a good agreement between computed and in-surface measured residual stresses. This is a result of a full simulation of the manufacturing process: quenching followed by machining and grinding of this component.

4.2. Impact of hydrotest on residual stress fields

Hydrotest has been simulated on a whole model of the nozzle including saddle and connecting pipes presented in Figure 14. The values of the connecting pipe lengths have been fixed to avoid any interaction effects with the end forces. The mesh of the new model contains 42331 linear elements.

The first step consists in the transfer of the results obtained on the saddle for quenching, machining and grinding simulation to the whole model. Residual stresses and plastic deformations are projected from the saddle to the same part in the new model. A new equilibrium state is computed on the whole model, changing the residual stress distributions in the more compliant parts, but not in the up-stream nozzle corner. Then, pressure is applied step by step onto the internal surface up to 1.8 times the design pressure which makes 31.05 MPa. This value is applied in the hydrotest of cast components at ambient temperature (RCC-M B5000, 2000). In the end, pressure is decreased to zero to get the residual stress fields after hydrotest. These computations are based on a von Misès yielding criterion, a kinematic strain hardening model material behavior law and on the small strain hypothesis.

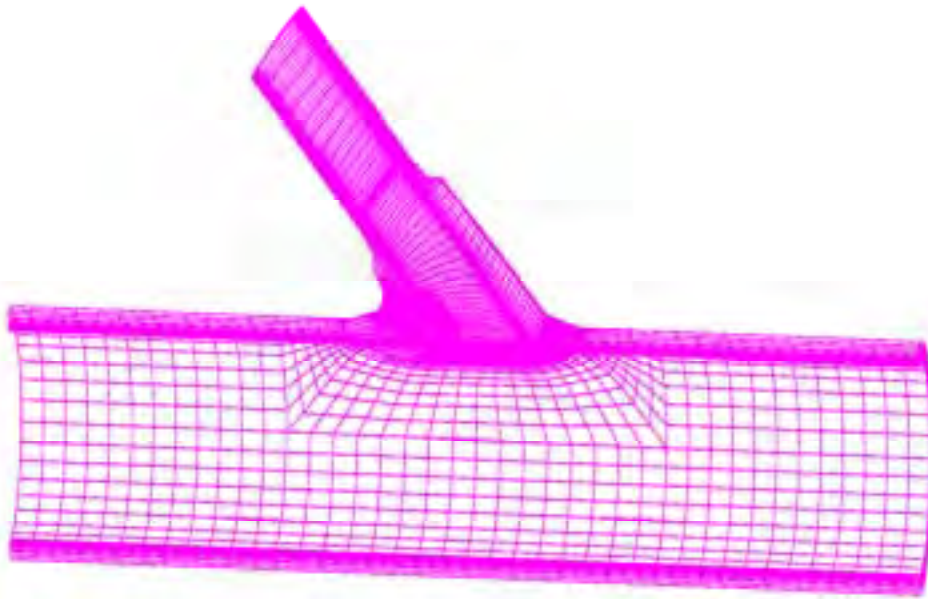


Fig. 14 Mesh of the entire nozzle

After hydrotest, residual stresses are relieved as shown in Figures 15a and 15b. The importance of this relaxation depends on the initial residual stress level and on the local geometry. The stress relaxation is the highest in the up stream part of the nozzle corner which is the most yielded under pressure increase. Eventually, the residual stress level does not exceed 80 MPa in the up stream part of the nozzle corner.

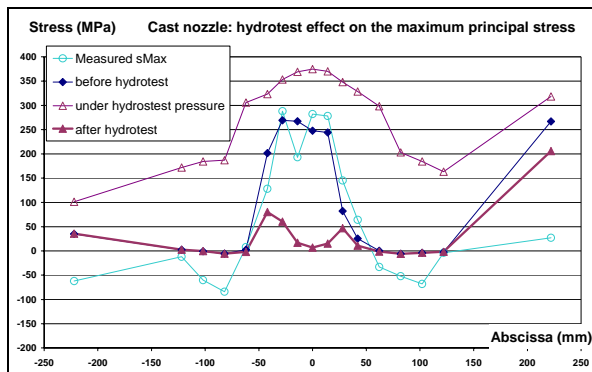


Fig. 15a Effect of hydrotest on maximum principal stresses

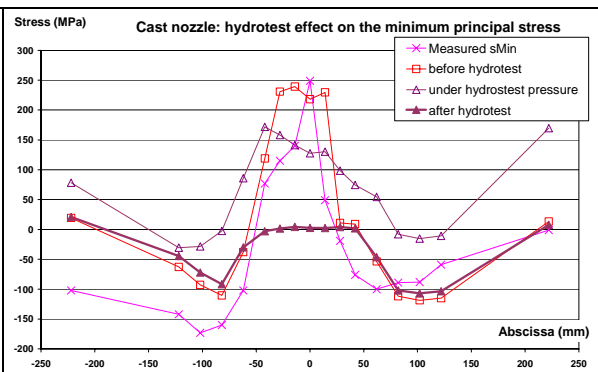


Fig. 15b Effect of hydrotest on minimum principal stresses

More details on the 3D finite element techniques used to simulate the whole manufacturing process of this cast duplex stainless steel nozzle as well as computed distortions and residual stresses during manufacturing and after hydrotest will be presented in a near future (Duranton, 2007).

5. CONCLUSIONS

These three types of analyses illustrate the importance of simulating the manufacturing processes for computing realistic residual stress fields. The simulation of a DMW welding has given excellent results provided that material characterization of the weld filler material is taken with great care, each elementary step of the mock-up manufacturing procedure is simulated and that all passes are computed. Simulating the quenching

process is much easier and gives reliable results. The more difficult task remains the machining or grinding simulations, since in many cases, the machining or grinding conditions are not well known. However, it has been observed in the welding and quenching analysis that surface measured residual stresses are essentially the result of machining or grinding, therefore such measurements cannot be used to infer residual stress distribution through the thickness. On the other side, welding or quenching simulation is of no help for the evaluation of surface residual stress fields, which play a determinant role in corrosion and fatigue initiation. More effort in the simulations should be devoted in surface state characterization and estimation of residual stress due to machining and grinding.

ACKNOWLEDGEMENTS

The authors would like to acknowledge ESI-group for their contribution in machining process simulations and Framatome-ANP engineers C. Bois, N. Safa, C. Petesch, C. Migné who have performed residual stress computations and discussed their results.

REFERENCES

- Fricke S., Keim E., Schmidt J., "Modeling of root formation during the welding process with the help of the 3D FE method", *Mathematical Modelling of Weld Phenomena 4*, Maney Publishing, 1998.
- Gilles Ph., "Residual Stress Problems in the Nuclear Industry", *CRBE seminar*, Troyes (FRA), March 6th 2002, to appear in Res. Stress Handbook, V2 Ch 2.2, Ed. T. Proulx, Bethel, USA .
- Gilles Ph., Pont D., Keim E., Devaux J., 2004, "Framatome-ANP experience in numerical simulation of welding", REEF, *Revue Européenne des Éléments Finis*, Vol. 13, 3-4, Hermes Ed., pp. 343-375.
- Cattant, F., De Bouvier, O., Economou, J., Tessier A. & Yrieix, B., 1994, "Examens et études métallurgiques de liaisons bimétalliques du circuit primaire principal", *Fontevraud III*, 12-16 sept. Vol. 1, p.125.
- EUR 20281 Report, 2001, "Mechanical Behavior of Dissimilar Metal Welds".
- Chas G., Faidy C., Hurst R., 2001, "Structural Integrity of Bi-Metallic Welds in Piping Fracture Testing and Analysis", ASME Pressure Vessel and Piping Conference, PVP 2001, Vol. 423, Atlanta, USA.
- Faidy C. et al., 2001, "Assessment of Aged Piping Dissimilar Metal Weld Integrity: ADIMEW", Proc. of FISA 2001 Conference, Luxembourg, EUR 20281.
- Faidy C. – "Structural integrity of dissimilar welds –ADIMEW project overview" *Proc. of PVP 2004, ASME Pressure Vessel and Piping Conference, 2004, USA*.
- Martin G. & Ménard A. – "Experimental Four Points Bending Test On A Real Size Bimetallic Welded Pipe: European Project ADIMEW" *Proc. of PVP 2004, ASME Pressure Vessel and Piping Conference, 2004, USA*.
- Wintle J. B., Goldthorpe M. – "Fracture analyses of the ADIMEW dissimilar metal weld test" *Proc. of PVP2004, ASME Pressure Vessel and Piping Conference, 2004, USA*.
- Gilles Ph., Devaux J., Faidy C. – "ADIMEW project: Prediction of the ductile tearing of a cracked 16" dissimilar welded junction" *Proc. of PVP2004, ASME Pressure Vessel and Piping Conference, 2004, USA*.
- Leggatt R. H., 1987, "Relaxation of residual stresses during post weld heat treatment of submerged arc weld in a C-Mn-Nb-Al steel" International Conference "Stress Relieving Heat Treatment of Welded Steel Constructions" Sofia, Bulgaria, 6-7 July 1987 – Proceedings pp 247-256.
- Ohms, C, Katsareas, D. , Wimporya, R., Hornak, P., Youtsos, A.G., 2004, "Residual stress analysis in a thick dissimilar Metal weld based on neutron diffraction", ASME PVP conference ASME / JSME Pressure Vessels and Piping Conference, July 25-29, San Diego, California, USA.
- Katsareas, D. , Ohms, C, Youtsos, A.G., 2004, "On the Performance of a Commercial Finite Element Code in Multi-Pass Welding Simulation", ASME PVP conference ASME / JSME Pressure Vessels and Piping Conference, July 25-29, San Diego, California, USA.
- Schindler, H. J., 2003, 'Residual stress effects on crack growth mechanisms and structural integrity', 9th Conf. on Mechanical Behaviour of Materials, Geneva, Switzerland, 25-29 May.
- RCC-M, 1997 & addenda 1998, 2000, "Design and construction rules for mechanical components of PWR nuclear islands", AFCEN, Paris
- Dupas, Ph., Le Delliou, P., Sussen, L., 1996, "Evaluation of quenching residual stresses in cast stainless steel pipe and elbow", ICRS4 conference, June, Cluny, France.
- RSE-M, 1997 & addenda 2000, « Surveillance and in-service inspection rules for mechanical components of PWR nuclear islands", AFCEN, Paris.
- Mc. Adams W. H., 1961, "Heat Transmission", MC Graw-Hill – Series in chemical engineering – Third edition.
- Faure, F., Leggatt, R. H., 1996, "Residual stresses in austenitic stainless steel primary coolant pipes and welds of pressurized water reactors", *Int. J. Pres. Ves. & Piping* 65, 265-275

RCC-M, 1997 & addenda 1998, 2000, “Design and construction rules for mechanical components of PWR nuclear islands”, AFCEN, Paris

Duranton, P., Devaux J., Gilles Ph., Petesch, C., Bergheau, J.-M., to appear in AMP, « 3D Modelling of Hyper-Hardening, Grinding and In-Use Conditions of an Austeno-Ferritic Stainless Steel Nozzle”, submitted to AMPT conference 2007.